

DOI:

Experimental investigation of the ignition, flame propagation and flashback behavior of a premixed green propellant consisting of N_2O and C_2H_4

Lukas Werling^{†*}, Felix Lauck*, Dominic Freudenmann*, Nicole Weber*, Helmut Ciezki*
and Stefan Schleichtriem*

*DLR (German Aerospace Center), Institute of Space Propulsion Lampoldshausen
Im Langen Grund 74239 Hardthausen

Lukas.Werling@dlr.de · Felix.Lauck@dlr.de

[†]Corresponding author

Abstract

Regarding the research on alternatives for monopropellant hydrazine, several so called green propellants are currently under investigation or qualification. Aside others, DLR's Institute of Space Propulsion investigates a N_2O/C_2H_4 premixed green propellant. During the research activities, flashback from the rocket combustion chamber into the feeding system has been identified as a major challenge when using the propellant mixture. This paper shows the results of ignition experiments conducted in a cylindrical, optical accessible combustion chamber. During the ignition and flame propagation process, pressure, temperature and high-speed video data were collected. Additionally flame arresting elements were tested on their ability to prevent flame flashback and critical Peclet numbers were derived. Due to the test results, sintered porous materials seem to be suitable as flashback arresters.

1. Introduction

Since decades hydrazine is used as a monopropellant to power satellites, landers or planetary probes. The versatile propellant offers good performance (I_{sp} up to 240 s), is long term storable and easy to decompose via catalyst. Further advantages are the cold start capability of hydrazine thrusters and the low risk of unwanted decomposition or explosion. Numerous years of experience with reliable hydrazine thrusters create space systems which are able to reach the edges of our solar system. A remarkable example is the Voyager 1 probe, which re-ignited its hydrazine thrusters after more than 30 years in the harsh environment of interplanetary space.³⁷ Nevertheless hydrazine and its derivatives have a very concerning attribute: They are highly carcinogenic and toxic. Due to the high toxicity, complex safety measures are needed which result in high handling and transportation costs. Thus hydrazine was recently put on the REACH (Registration, Evaluation, Authorization and Restriction of Chemicals) list for substances with very high concern.¹³

Due to those drawbacks of hydrazine during the last decade the research on less or non toxic alternatives came more and more in the focus of investigations across the world.^{4,16,19} Several so called Green Propellants are currently under investigation or qualification: ADN based monopropellants (LMP-103S, FLP-106),^{1,2,31} HAN-based propellants (AF-M315E),^{26,32-34} H_2O_2 ^{6,7,20,43} and mixtures of N_2O with different hydrocarbons, also known as nitrous oxide fuel blends.^{29,45} Aside other propellants and propellant combinations, DLR's Institute of Space Propulsion investigates a N_2O/C_2H_4 premixed green propellant in an experimental combustion chamber.^{2,44} During the research activities, flashback from the combustion chamber into the feed system has been identified as a major challenge. This challenge must be met to assure a safe use of the propellant mixture. Thus the flame flashback and ignition behavior of the propellant has to be understood.

To investigate the behavior during ignition and flame propagation, a cylindrical, optical accessible combustion chamber was constructed and implemented in a test setup for premixed propellants. Furthermore several flame arresting elements (porous materials) were tested on their ability to prevent flame propagation from the ignition chamber into a secondary (flashback) chamber. A commonly used parameter to compare the different conditions under which a flame flashback occurs is the dimensionless Peclet number.^{25,27,42} For the used porous materials the critical Peclet number under which flashback occurs, are to be derived. The experimental data about the possible operation ranges should help designing future flashback arresters. During the ignition and flame propagation process, pressure, temperature

IGNITION, FLAME PROPAGATION AND FLASHBACK BEHAVIOR OF A N₂O AND C₂H₄ GREEN PROPELLANT

and high-speed videos data are recorded. To test the quenching limits of the flashback arresters, the ignition pressure is raised step by step until a flashback occurred. The pressure data and the high-speed images should later be used for comparison with numerical simulations of the combustion process inside a closed volume.

2. Theoretical background - flame propagation, flashback and quenching

During ignition and flame propagation in a closed volume several effects influence the flame velocity and the flashback or quenching behavior of the flame. The following section describes the effects observed during the combustion tests and gives a general overview.

2.1 Reaction mechanism

The overall chemical reaction for a stoichiometric N₂O/C₂H₄ mixture is given by:



To calculate the laminar flame speed a Cantera-Script¹¹ and a GRI3.0 reaction mechanism³⁶ was used. The reaction mechanism was derived by the Institute of Combustion Technology at DLR in Stuttgart. Compared to the adapted/extended mechanism mentioned in their paper,⁴¹ an improved, reduced set of reactions was available for calculation. This mechanism predicts the laminar flame speed of the experiments with an approximate error of $\pm 5\%$.

2.2 Flame propagation in a closed volume

The flame front in a closed volume moves with an average speed that is several times larger than the laminar flame speed. This is caused by the rapid expansion of the burned gases behind the flame front. Thus the observed flame propagation speed S_{ofp} result from the laminar flame speed S_L and the expansion speed of the combustion products S_{Exp} :

$$S_{ofp} = S_L + S_{Exp} \quad (2)$$

Using energy and mass conservation, for a one dimensional isobaric flame propagation, the expansion speed of the combustion products results to:³⁰

$$S_{Exp} = \frac{\rho_u - \rho_b}{\rho_b} S_L \quad (3)$$

Here ρ_u marks the density of the unburned mixture and ρ_b the density of the burned mixture. Due to high density changes across the flame front, the expansion speed of the combustion products is significantly higher than the laminar flame speed. Using equation (3) and equation (2) the observed flame propagation speed results to:

$$S_{ofp} = \frac{\rho_u}{\rho_b} S_L \quad (4)$$

Depending on geometry and the pressure inside the combustion chamber, the flame propagation speed changes during the combustion process. For a constant volume combustion in a spherical bomb, the laminar flame speed can be derived by the pressure development in the closed volume P related to the initial pressure P_0 , the change of burned mass fraction $Y = \frac{m_b}{m_0}$, the radius of the spherical volume R_W and the isentropic coefficient κ :

$$S_L = \frac{R_W}{3} \left(1 - (1 - Y) \left(\frac{P_0}{P} \right)^{\frac{1}{\kappa}} \right)^{-\frac{2}{3}} \left(\frac{P_0}{P} \right)^{\frac{1}{\kappa}} \frac{dY}{dt} \quad (5)$$

A good overview of different approaches to determine the laminar flame propagation speed in a spherical, closed volume can be found in the paper by Faghii and Chen.¹⁴

2.3 Flame Flashback

Flame flashback in a premixed combustible mixture can generally be caused by two effects: In the first case the flow field in which the flame burns allows the flame to propagate upstream. In the second case the flame heats up a surface and the hot surface causes ignition of the mixture upstream the flow. Four general flashback mechanisms are distinguished:¹⁷

IGNITION, FLAME PROPAGATION AND FLASHBACK BEHAVIOR OF A N₂O AND C₂H₄ GREEN PROPELLANT

- Flame flashback in the core flow
Here the flame speed is larger than the main flow speed and the flame can propagate contrary to the main flow.
- Flame flashback in the boundary layer
In this case the velocity gradient at the boundary layer is larger than the temperature gradient caused by flame quenching effects. So the flame speed is larger than the flow speed at a distinct distance from the wall. In this zone the flame can propagate upstream.
- Flame flashback caused by combustion instabilities
Due to pressure oscillations in the combustion chamber, the flame can be pushed forth and back. If the instability in the combustion chamber rises above the feeding line pressure, the flame can propagate backwards upstream the injection system. During transient phases such as during shutdown or ignition of an engine or motor, this is the main reason for occurrence of flashback. To avoid flame flashback, caused by a pressure peak at ignition, the premixed flame has to be quenched by an appropriate flashback arrester.
- Flashback caused by swirls in the combustion chamber
If large eddies and recirculation zones are present in the combustion chamber, the vortices can lead to a reversed flow of the combustible products. Due to heating of the injector walls, the quenching diameter decreases. Additionally the return flow influences the boundary layer, so the local flow speed is reduced and flame flashback is supported.

2.4 Flame Quenching

The dimensionless Peclet number is often used to describe if a flame is able to propagate through a small gap or hole. Several assumptions are made to derive the dependency of characteristic combustion parameters and the corresponding diameter or distance: The combustion products behave as an ideal gas, the pressure across the reaction zone is constant, the heat conduction is infinite fast, the flame structure is laminar and the walls are not heated by the flame. Via energy conservation, mass conservation and the ideal gas law, the critical quenching diameter d_q can be written as:^{27,42}

$$d_q = \frac{Pe_c \cdot \alpha_u}{S_L} \quad (6)$$

Here Pe_c is the critical Peclet number under which quenching occurs, S_L marks the laminar flame speed and α_u is the thermal diffusivity of the unburned mixture:

$$\alpha_u = \frac{\lambda_u}{\rho_u \cdot c_{p,u}} \quad (7)$$

In this equation, the heat conductivity of the unburned mixture is represented by λ_u , the density of the unburned mixture by ρ_u and the specific heat capacity of the unburned mixture by $c_{p,u}$. In literature the critical Peclet number varies widely with the used test setup and the corresponding quenching phenomena. Furthermore the wall material seems to play a role in defining the quenching distance. Different Peclet numbers are derived for:

- Head on quenching
For a propane/air mixture the critical Peclet number observed in experiments ranges from 3.8 - for quenching at ceramic walls to $Pe_c = 4.7$ for quenching at polished steel walls.³ Boust et. al obtained critical Peclet numbers of 2.6 for a steel obstacle.⁵
- Side wall quenching
The critical Peclet number ranges from 5.6 for ceramic walls to 8.5 for polished steel walls, for a propane/air mixture.³ During other experiments a Peclet number of 4.5 was derived.⁵
- Quenching between parallel plates
For quenching between parallel plates, the critical distance seems to be 0.65 time the distance of the quenching diameter in circular ducts.¹⁵ In a study of Jarosinsky²³ for wedged shaped channels the Peclet number was observed to be 42, while the value for rectangular channels was 51. In a numerical study, Daou and Matalon¹⁰ found the critical quenching distance in a two-dimensional channel corresponding to 15 times the flame thickness. This is equivalent to a Peclet number of 15. It has to be considered that in the study of Daou and Matalon only conductive heat losses were simulated and the flow was assumed to be laminar and stationary (Poiseuille-flow).

IGNITION, FLAME PROPAGATION AND FLASHBACK BEHAVIOR OF A N₂O AND C₂H₄ GREEN PROPELLANT

- Quenching in circular ducts
Spalding³⁸ made a few assumptions about the reaction behavior and calculated a critical Peclet of 60.5 for quenching in ducts. While Zel'dovich found the critical Peclet number to be approximately 65.²⁷ For porous materials the critical Peclet number seems to be in a range of $\pm 50\%$ regarding the theoretical value of 60.5.^{8,24}

Despite the wide range of experimentally and numerically derived Peclet numbers, the quenching diameter generally scales with a characteristic flame length scale δ_L .

$$\delta_L = \frac{\alpha}{S_L} \quad (8)$$

A good summary of the different Peclet numbers can be found in the textbook "Combustion Phenomena" by Jarosinski and Veyssiere.²⁵

3. Experimental setup and test procedure

The experimental setup is located at the M11 test bench at DLR in Lampoldshausen. It consists of a flexible feeding system for the gas supply, a mixing section and the test chambers.

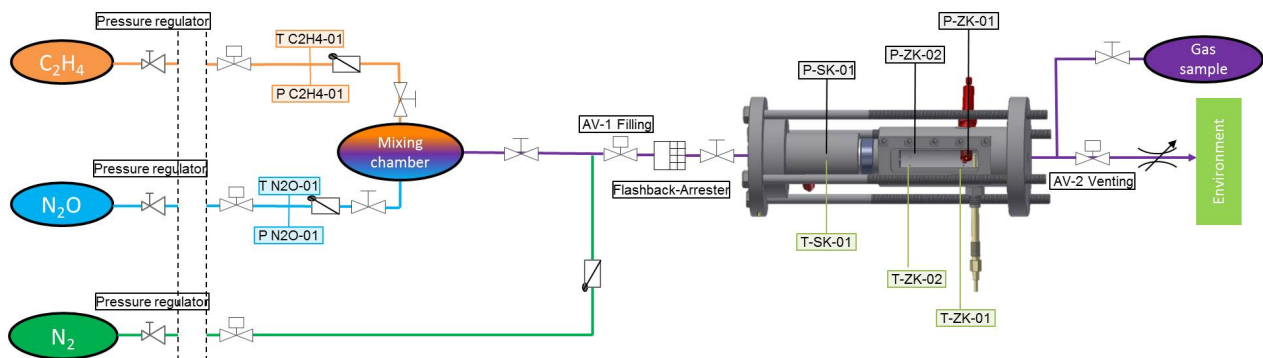


Figure 1: Simplified P&ID of the test setup

A simplified P&ID of the test setup is shown in figure 1. On the left side of the instrumentation diagram, the gas supply tanks are shown. Downstream the tanks pressure regulators are situated to adjust the oxidizer or fuel pressure. Furthermore each feeding line is equipped with an automatic valve and pressure sensors. The pressure sensors are used to compare the manually adjusted pressure at the regulators with the pressure in the supply lines. Additionally the gas temperature is measured via Typ-K thermocouples. The pressure and temperature data are used to calculate the wanted mixture ratio in the mixing chamber. Due to this calculation the pressure of the second gas could be adjusted. The mixing chamber is separated to the ignition and flashback chamber via two valves and a commercial available flashback arrester.

At the ignition chamber (chamber with window) two pressure transducers (Kistler Typ 4045, 100 bar, P-ZK-01, P-ZK-02) and two type-K thermocouples (T-ZK-01, T-ZK-02) are mounted. The flashback chamber is equipped with one pressure sensor (Kistler Typ 4045, 100 bar, P-SK-01) and also a typ-K thermocouple (T-SK-01). The data acquisition rate of the pressure sensors is 50 kHz, the thermocouples are recorded with 100 Hz. Due to the slow response time of the thermocouples, they are only used for detection of the flashback. The signals of the thermocouples and pressure transducers are amplified via Dewetron (DAQP-STG) signal amplifiers. The measurement system consists of a Jäger Adwin ProII processor with corresponding modules for signal acquisition and valve controlling. To ignite the gaseous mixture, a standard car spark plug or a glow plug could be used. The inner diameter of the ignition chamber is 25 mm, while the length of the cylindrical combustion volume is 93 mm.

The high speed camera used for the video acquisition of the ignition and combustion process is a Photron Fastcam SA1.1. The frame rate was set to 62500 fps with an resolution of 448x176 pixels.

On the downstream side of the ignition chamber an automatic valve for venting the chamber prior and after to the tests is mounted. Additionally a fitting and a valve for gas sampling is available. A photo of the mounted test chamber is shown in figure 2(a). In figure 2(b) the sectional view of the chamber with a mounted porous material can be seen.

3.1 Test procedure

The process of test preparation and test conduction is shown in figure 3. Prior to the mixing of the gases, the intended mixture ratio was calculated via Matlab script. The real gas data were obtained from Refprop database, taking the

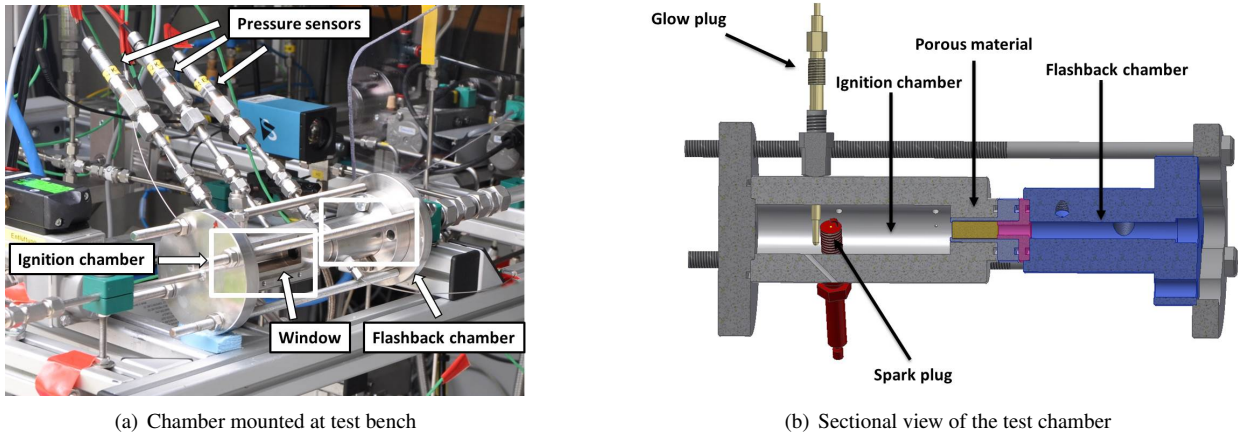
IGNITION, FLAME PROPAGATION AND FLASHBACK BEHAVIOR OF A N_2O AND C_2H_4 GREEN PROPELLANT

Figure 2: Ignition and flashback chamber

given ambient temperature into account. For the mixing of the two gases an ideal gas mixing behavior was assumed. The mixture ratio was set according to the following relationship:

$$\phi = \frac{ROF}{ROF_{stoich}} = \frac{\frac{m_{N_2O}}{m_{C_2H_4}}}{\left(\frac{m_{N_2O}}{m_{C_2H_4}}\right)_{stoich}} = \frac{\rho_{N_2O} \cdot V_{mix}}{\rho_{C_2H_4} \cdot V_{mix}} \cdot \frac{1}{9.41} \quad (9)$$

The first step during the test procedure, was filling of the mixing vessel with C_2H_4 at an absolute pressure of 6 bar. To clarify the calculation, the resulting densities and pressure levels are shown here for a gas temperature of 293 K.

At 6 bar and 293K the density of C_2H_4 is $\rho_{C_2H_4-6bar} = 7.17 kg/m^3$. Assuming ideal gas mixing, the corresponding N_2O density ρ_{N_2O} was set to 10.5 ($\phi = 0.9$) times the C_2H_4 density at 6 bar $\rho_{C_2H_4-6bar}$. An additional density of $\rho_{N_2O} = 75.29 kg/m^3$ had to be added to the mixing tank to obtain the wanted mixture ratio.

$$\rho_{N_2O} = \rho_{N_2O_{xbar}} - \rho_{N_2O_{6bar}} \quad (10)$$

The needed N_2O density $\rho_{N_2O_{xbar}}$ was calculated and the corresponding pressure ($xbar$) was obtained from Refprop.¹²

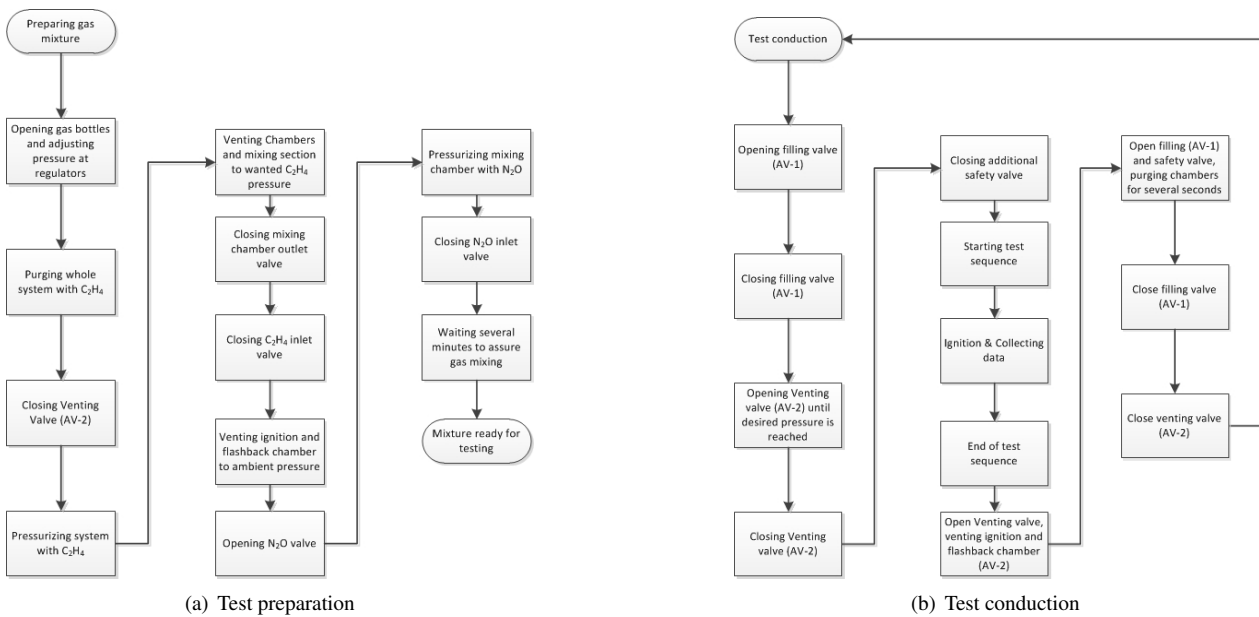


Figure 3: Test preparation and conduction

In this case the required N_2O pressure was 35.9 bar. After the mixing tank was filled with N_2O , all valves were closed

IGNITION, FLAME PROPAGATION AND FLASHBACK BEHAVIOR OF A N₂O AND C₂H₄ GREEN PROPELLANT

and the gases were allowed to mix "for the duration of a coffee". Subsequent to this highly reproducible time interval, the mixture was ready for testing. All tests were conducted according to figure 3(b).

Directly after filling and mixing the gases, a gas sample was collected. A second gas sample was taken at the end of a whole test run, when the mixing tank was nearly empty. Thus the variation of the mixture ratio and the possible pollution of the ignitable mixture with exhaust gases could be detected.

At the beginning of the experimental campaign, several tests were performed to adjust the shutter time of the high-speed camera and to assure proper function of the data acquisition system. During those tests no porous materials were mounted. The propagation speed of the flame depending on different ignition pressure was observed during this test runs.

3.2 Used Porous materials

During the flashback tests, two different types of porous materials were used: SIKA-R sintered stainless steel filters (material 1.4404) and SIKA-B sintered bronze filters (material 2.1052) manufactured by GKN sinter metals. The materials were available in different lengths and filter grades. An overview of the used materials is given in table 1.

Table 1: Used porous materials

Material	Filter grade	length [mm]	Pore Size ^{a18} [mm]
SIKA-B, 2.1052	200	21	0.573
SIKA-B, 2.1052	150	21	0.344
SIKA-B, 2.1052	150	10.5	0.344
SIKA-B, 2.1052	100	21	0.232
SIKA-B, 2.1052	30	10.5	0.066
SIKA-R, 1.4404	200	21	0.286
SIKA-R, 1.4404	200	10.5	0.286
SIKA-R, 1.4404	200	7	0.286

^a DIN ISO 4003

Different lengths and filter grades were chosen to investigate the influence of the length, the pore size and to examine the influence of the filter material itself on its quenching ability. Pressure drop tests for the different porous materials were conducted prior to this study.²⁸ During those tests the SIKA-B material shows a reduced pressure drop for a similar pore size compared to the SIKA-R material. Additionally the SIKA-B material offers a higher heat conductivity, this could improve the quenching behavior. Two of the used porous materials are shown in figure 4



Figure 4: SIKA-R (left) and SIKA-B material (right)

4. Results and discussion

Ignition tests were conducted in different configurations: With flashback-arresters mounted, without flashback arresters, with a quartz glass window at the side of the ignition chamber and with steel plates instead of the glass window to perform tests at higher pressure levels.

IGNITION, FLAME PROPAGATION AND FLASHBACK BEHAVIOR OF A N_2O AND C_2H_4 GREEN PROPELLANT

Pressure and temperature data were collected during all tests. The thickness of the glass window was 5 mm, during the tests the window could withstand a ignition pressure of approximately 1.8 bar. At higher ignition pressure levels the glass did burst due to large pressure peaks during the combustion process (see e.g. figure 10(a)). Thus high-speed video images are only available for tests with ignition pressure levels below 1.8 bar.

4.1 Tests without flashback arresters/porous materials

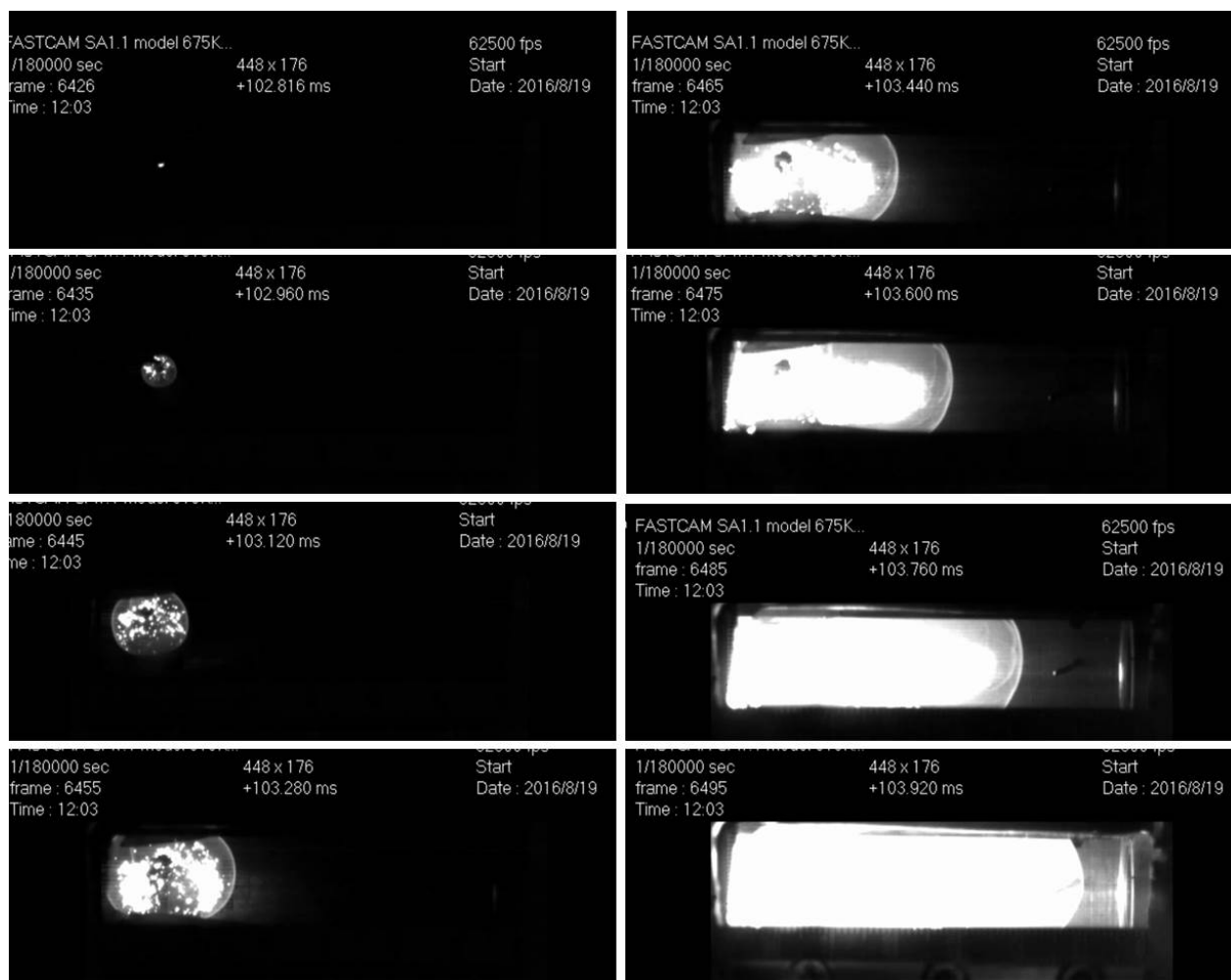


Figure 5: Typical images of high speed video during test run (62500 fps; despite the first gap, every 10th frame was taken; time distance in between frames= $160 \mu s$, 1bar ignition pressure)

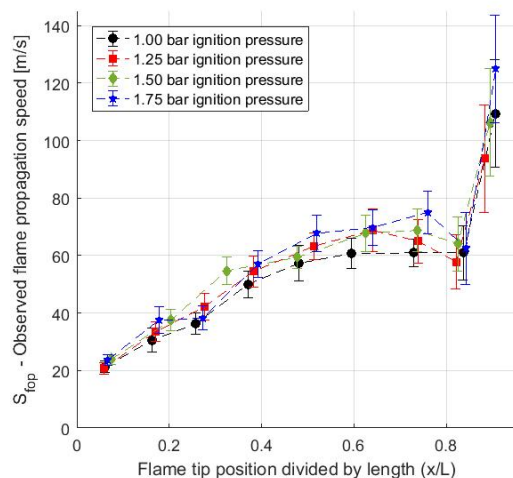
Typical frames of the flame propagation in the ignition chamber are shown in figure 5. The first image shows the ignition of the mixture caused by the spark plug. Concerning the flame propagation and shape of the flame front, the following steps are observed during the experiments:

- Ignition of the combustible mixture. The flame forms a sphere around the point of ignition.
- The flame front approaches the walls of the chamber. Flame shape changes from spherical form to a "finger like" form. The tip of the flame is accelerated in axial direction.
- The upper and lower flame edge touch the combustion chamber walls, there the flame is quenched. The reacting flame front moves horizontally.

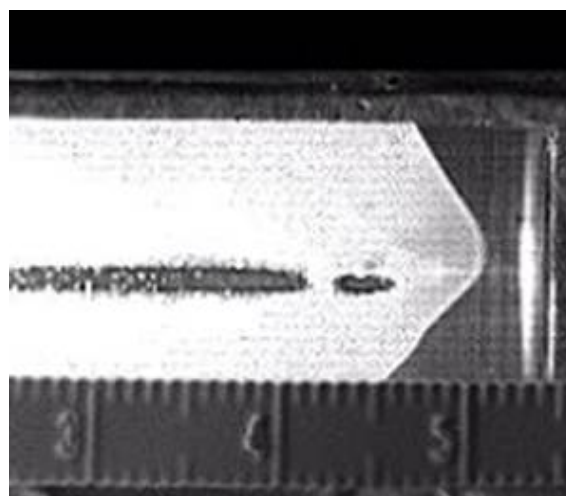
The observed effects and phases during ignition and flame propagation agree well with effects described in literature.^{9,39,40} The glowing particles which are visible behind the flame front are soot particles caused by pollution of the ignition chamber due to previous tests. The video data was used to calculate the observed flame propagation speed. To

IGNITION, FLAME PROPAGATION AND FLASHBACK BEHAVIOR OF A N_2O AND C_2H_4 GREEN PROPELLANT

derive the flame velocity the visible distance on the camera was correlated to the number of pixels on the image. Figure 6(a) shows the observed flame propagation speed during tests without flashback arresters at different ignition pressure levels.



(a) Flame propagation speed for different ignition pressures



(b) Acceleration of flame tip at constriction

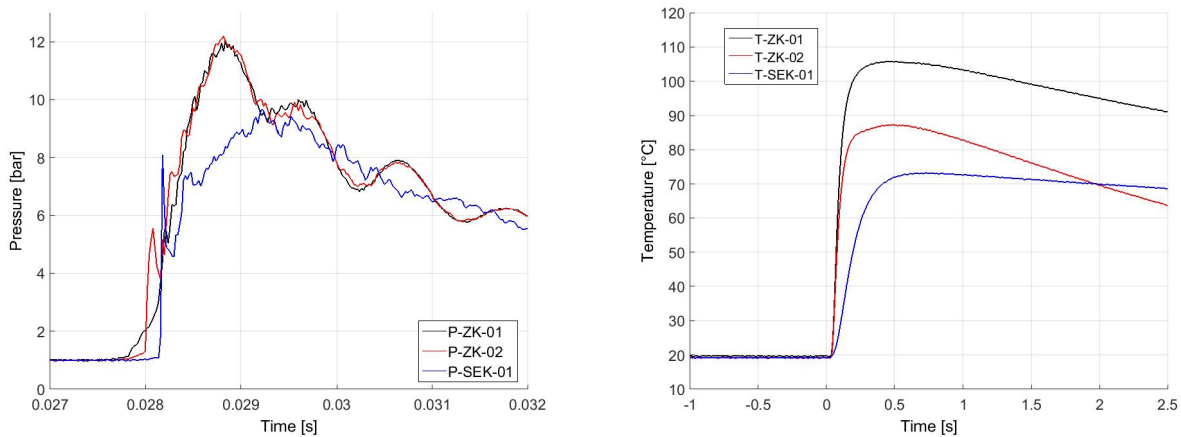
Figure 6: Flame speed in ignition chamber and flame entering the constriction

The following behavior was observed during analysis of the flame propagation velocities:

- The flame starts to accelerate, beginning at the point of ignition. The acceleration seems to be linear until the flame tip reaches the middle ($x/L \approx 0.5$) of the observed volume.
- After approximately half the length of the chamber ($x/L \approx 0.5$) a "velocity plateau" is reached. The flame travels at a quite constant speed. This effect is possibly caused due to a relatively constant surface area of the "finger shaped" flame front.
- At the right end of the chamber ($x/L \approx 0.8$) the flame speed slightly drops. Two effects might influence this behavior: First the unsymmetrical position of the spark plug in the ignition chamber causes the flame front to propagate to the right (visible through window) and to the left. The left edge of the combustion chamber is reached earlier due to the position of the spark plug (see figure 2(b)). When the left flame front reaches the wall, the flame surface is reduced significantly. Second the flow field ahead of the right flame front might interact with the walls at the constriction and slow down the flame tip.
- When the flame approaches the constriction in between the ignition and flashback chamber, it starts to accelerate sharply. This is caused by an acceleration of the subsonic flow at the constriction. Figure 6(b) shows the acceleration of the flame tip while entering the connection in between the two chambers.
- For higher ignition pressures the average flame propagation speed seems to be larger. Despite the laminar flame speed decreases with rising pressure,⁴¹ the mass consumption of the flame for a higher pressure/density increases.²² The increase in unburned gas density exceeds the decrease in laminar flame speed, thus the flame propagation speed is rising with higher ignition pressure.

Pressure and temperature data were collected during the test runs. Figure 7(a) and figure 7(b) show the pressure respectively the temperature data during a test with an ignition pressure of 1 bar and no flashback arresting element mounted.

In this case the overpressure caused by the combustion in the closed vessel reaches 12 times the ignition pressure. The pressure peak during the combustion process is very short, thus the thermocouples can not resolve the temperature during the flame propagation. Additionally the position of the pressure transducers during the test with mounted windows was not ideal. The compression of unburned gases and the time delay caused by the long connecting tubes (see figure 2(a)) distort the pressure values measured in the chamber. This was realized during later tests without the glass window, when the sensors were mounted directly at a steel plate which replaced the glass window. Those tests resulted in a much better resolution of the pressure development inside the closed vessel. Nevertheless, figure 7(a)

IGNITION, FLAME PROPAGATION AND FLASHBACK BEHAVIOR OF A N₂O AND C₂H₄ GREEN PROPELLANT

(a) Pressure course during ignition tests without flashback arrester

(b) Temperature course during ignition test without flashback arrester

Figure 7: Pressure and temperature data for an ignition test without flashback arrester

shows that the initial pressure rise is measured by P-ZK-01 which is positioned next to the spark plug. This peak is followed by a pressure increase at P-ZK-02 and finally the sensor in the flashback chamber measures the pressure rise (P-SEK-01).

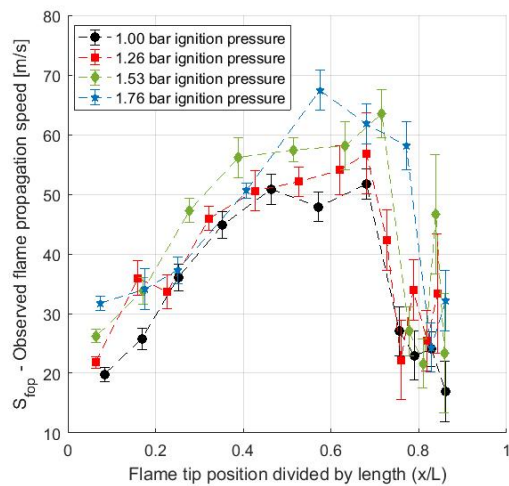
Regarding the thermocouples, the differences in the peak values are most likely caused by their position. The flashback chamber's volume to surface ratio is much lower than the ratio of the ignition chamber (diameter of the flashback chamber is 15 mm compared to 25 mm). Thus a less amount of gas is burned in the flashback and the heat produced by the chemical reaction can easier be conducted to the chamber walls. This finally results in a lower maximum temperature measured by T-SEK-01. The difference of T-ZK-01 and T-ZK-02 concerning the maximum temperature value might also be caused by their different positions. T-ZK-01 is located near the center of the ignition chamber, T-ZK-02 is placed near the constriction (the thermocouple can be seen in figure 8(b)).

4.2 Tests with porous materials as flashback arresters

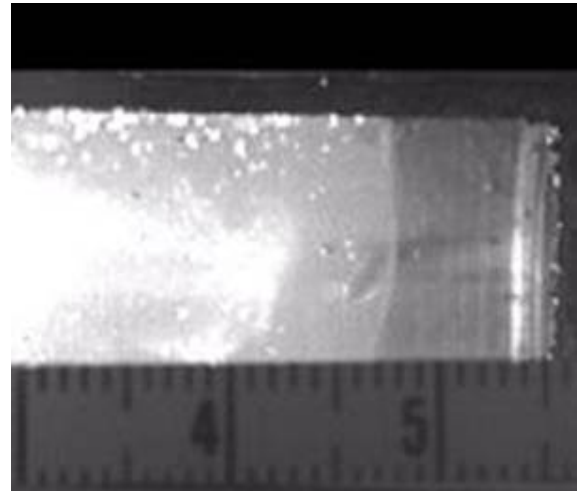
Subsequent to the tests without flashback arresting elements, combustion tests with porous material were conducted. At the beginning of each test series, the ignition pressure was set to 1 bar and successively raised until a flashback occurred. Up to a pressure of 1.8 bar the ignition and combustion process could be filmed via high speed camera. Pressure levels higher than 1.8 bar were conducted with steel plates mounted at the window's position on the ignition chamber. Figure 8(a) shows the flame propagation speed versus the chamber length during the tests up to 1.76 bar.

In contrast to the above shown velocity without an arresting element mounted, the flame propagation speed develops differently:

- At the beginning, the flame propagates spherically, the acceleration seems to be linear
- Approximately at $x/L \approx 0.4$ the flame speed reaches a velocity plateau. This plateau is reached earlier than in those tests without flashback arresters. The propagation of the flame and the expansion of the combustion products push the unburnt gas to the front of the porous material. From the flames point of view the material behaves similar to a solid wall, the flow is stopped or strongly slowed down in front of the porous structure. Because the observed flame propagation is mainly caused by the flow field's velocity (see equation 2), the flame velocity also drops.
- The flame propagation speed drops radically when the flame approaches the flashback arrester ($x/L \approx 0.7$). As mentioned above, the porous material causes the flow to stop in front of the flashback arrester. The flame propagation speed is mainly caused by expansion and flow of the hot combustion products. So if the speed of the flow field inside the chamber decreases, the flame front velocity also decreases.
- In some cases the flame seems to accelerate again after slowing down. The videos of those cases show, that the flame front was pushed forward by rapidly expanding gases in the connection tubes of the ignition chamber (expansion of gases in venting lines, tubes to pressure transducers, etc.). It is assumed that in some cases the

IGNITION, FLAME PROPAGATION AND FLASHBACK BEHAVIOR OF A N₂O AND C₂H₄ GREEN PROPELLANT

(a) Flame propagation speed with Flashback arrester for different ignition pressures

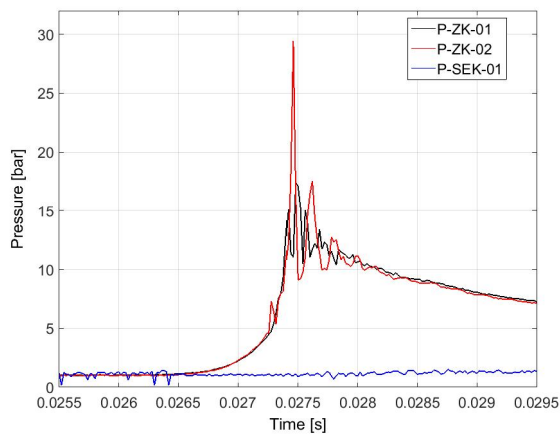


(b) Deacceleration of flame tip at flashback arrester

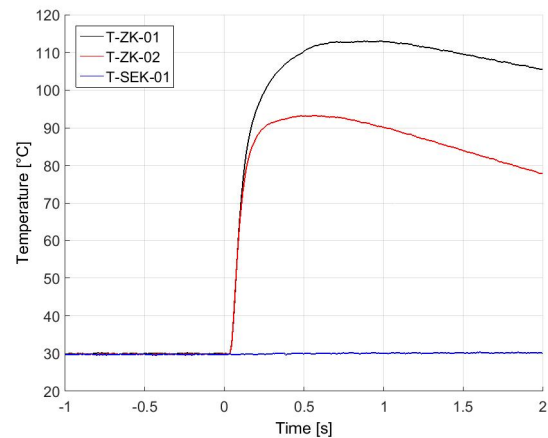
Figure 8: Flame speed in ignition chamber and flame in front of flashback arrester

deflagration in the connecting tubes undergoes a deflagration to detonation transition (DDT), so the combustible gas in those connections is consumed very quickly and pushes the flame in the main chamber forward.

The pressure data of the tests with mounted porous materials show different pressure peaks compared to the pressure peaks observed during the test without flashback arresters. This is caused by a different position of the pressure sensors: For the tests of figure 10(a) and 9(a) the pressure transducers in the ignition chamber were mounted at the steel plate, during the test of figure 7(a) the sensors were mounted at tubes above the ignition chamber (see also photo 2(a) for the initial sensor's position). Figure 7(a) shows the pressure course for an ignition pressure of 1 bar and figure 9(a) shows the corresponding pressure course for a test with identical ignition pressure. Differences in the maximum pressure values are most likely caused by the sensor position. As mentioned before, the absolute value of the pressure is not very



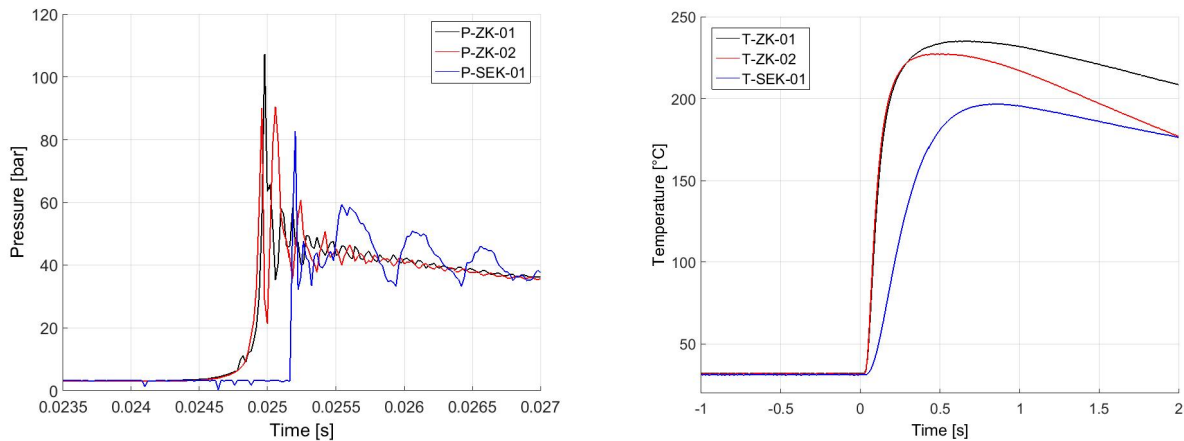
(a) Pressure in ignition and flashback chamber with porous material mounted - no flashback



(b) Temperature data - no flashback

Figure 9: Pressure and temperature for ignition tests with porous flashback arrester mounted and no flashback event

meaningful due to the shortness of the pressure peak. Figure 9(a) and figure 9(b) show the measurement data for a test where the flashback arrester worked properly and no flashback event was observed. In comparison the data in figure 10(a) and figure 10(b) show a flashback event. The sudden rise in temperature and pressure in the flashback chamber (blue lines) is a clear indicator that a flame flashback did occur. The time scale in between the maximum pressure peak in the ignition chamber and the corresponding pressure maximum in the flashback chamber seems to be in the range

IGNITION, FLAME PROPAGATION AND FLASHBACK BEHAVIOR OF A N₂O AND C₂H₄ GREEN PROPELLANT

(a) Pressure in ignition and flashback chamber with porous material mounted - no flashback

(b) Temperature data - no flashback

Figure 10: Pressure and temperature for ignition tests with porous flashback arrester mounted and flashback event

of 250 μ s. Due to shortness of this time interval it is assumed that the flame directly propagates through the porous material and immediately lights the mixture on the upstream side of the flashback arrester. During all conducted tests in which flashback was observed, the time delay in between the pressure maxima in the ignition and flashback chamber was smaller than 500 μ s. In comparison, the pressure in the ignition chamber was higher than the pressure in the flashback chamber for up to 100 ms. Comparing both time scales it seems to be most likely that flashback during the observed cases is caused by flame propagation through the material and not by a flow of hot combusted gases through the material. Thus the authors assume that no flashback caused by back flow of hot combustion gases occurred during the tests.

4.3 Critical Peclet numbers

During the combustion test with porous materials, the ignition pressure was raised step by step until a flashback was observed. Unfortunately during the test campaign no vacuum pump was available, so the minimum ignition pressure was approximately 1 bar. Due to this reason, for several coarse materials flashback was observed at the first ignition. A further restriction was given by the maximum ignition pressure. Increasing the static pressure above 4 bar and igniting the mixture resulted in a blow off of the used graphite seals due to the high pressure peaks. Several materials were able to stop the flame at this high pressure levels. So the final pressure at which those materials fail could not be derived. Nevertheless a minimum and a maximum Peclet number for the corresponding materials could be obtained. Figure 11 shows the corresponding Peclet numbers. The numbers were calculated using the following equation:

$$Pe = \frac{d_q \cdot S_L}{\alpha_u} \quad (11)$$

As described above, the laminar flame speed S_L was calculated via a Cantera script¹¹ and a reaction mechanism derived by DLRs institute of combustion technology.⁴¹ The thermal diffusivity for the unburned mixture α_u was obtained from Refprop database¹² assuming the mixture ratio which resulted from the gas chromatography. Figure 11 shows the derived Peclet numbers for the tested materials. For the SIKA B200 and B150 materials, the Peclet number where flashback was prohibited could not be observed. The flame passed the material at an ignition pressure of 1 bar. For the SIKA B30, the R 200 with 21 mm length and the R 200 with 10.5mm length, the Peclet number under which flashback occurs, could not be derived. For those materials the ignition pressure could not be raised high enough to observe flashback. For the two other samples (SIKA B100 21mm length and SIKA R200 7 mm length) the range of the Peclet numbers could be localized. The upwards facing triangles in the diagram show the maximum Peclet number at which no flashback occurred. The downwards facing triangles mark the Peclet number at which flashback occurred.

Although the upper and lower limits of the Peclet numbers could not be derived for all materials, general trends and limitations are visible.

- The porous sintered bronze material (SIKA B) seems to allow the flame passing at significantly lower Peclet numbers. Assuming the same pore diameter, the sintered bronze seems not to be able to quench the flame

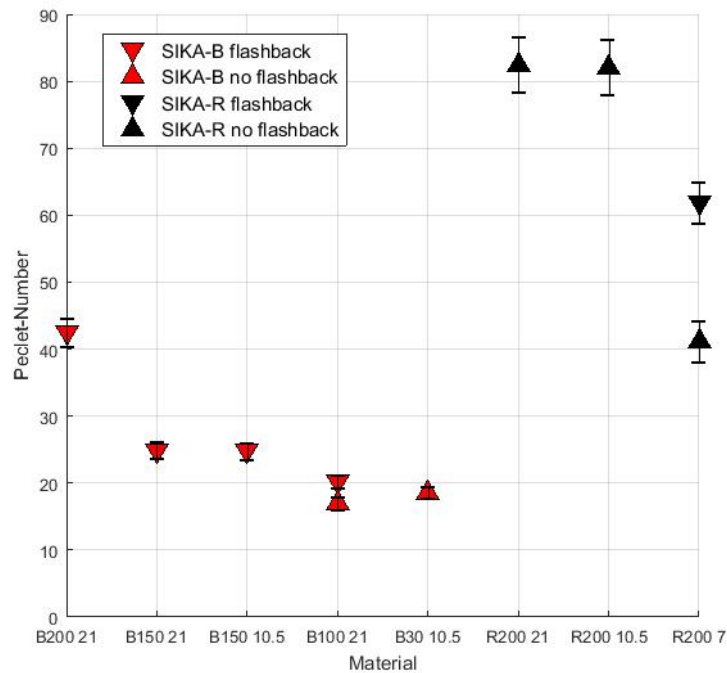
IGNITION, FLAME PROPAGATION AND FLASHBACK BEHAVIOR OF A N₂O AND C₂H₄ GREEN PROPELLANT

Figure 11: Pelet number with and without flashback for investigated porous materials

as good as the sintered stainless steel. The considerable smaller quenching Pelet number may be caused by catalytic effects of the copper based bronze material.³⁵

- b) Despite the analytic deviation of the quenching diameter, the length of the quenching channel seems have an influence. The shorter SIKA R 200 materials quenches the flame not as efficient as the longer materials. Due to the complex structure of the porous materials it may also be possible, that the largest pore in longer materials is smaller. However the length seems to have a significant influence on the quenching Pelet number. Regarding literature²¹ a proper flashback arrester needs to have an effective passageway length to quench the flame definitely. An empirical correlation for designing flashback arresters is given by:

$$L > 2S_t \cdot d_q^2 \quad (12)$$

Here L marks the flame arresters passageway length, S_t is the turbulent flame speed and d_q the quenching diameter of the passageway. The unit for L and d_q is cm , while the flame speed is in m/s . Equation 12 is used taking the pore size of the SIKA R 200 material as d_q . Furthermore a conservative estimation of the flame propagation speed during a test with an ignition pressure of 2 bar (at this point the SIKA R 200 material did quench the flame) is made. It is assumed that the turbulent flame speed in equation 12 corresponds to the flame propagation speed observed during the conducted tests. With an rough approximation of $S_t = 100m/s$ and $d_q = 0.0286cm$ L should be larger than $0.164cm$. The materials length is $0.7cm$, thus it should definitely quench the flame. Compared to the SIKA B material, the more complex pore structure of the SIKA R material possibly enhances the ability to quench the flame. Due to not uniform pore structure of the SIKA-R material, the pressure drop of those material is also higher than the pressure drop of the SIKA-B material. Furthermore the pressure drop across the material might influence the quenching Pelet number as well. It is thinkable that an increased pressure drop across the materials results in a larger quenching diameter.

4.4 Errors and Deviations

Different errors are assumed or were determined for the results of the Pelet numbers, for the pressure and temperature data as well as for the flame propagation speed.

First the flame propagation speed's error is examined. Due to the uncertainty of the correct pixel position and the manual determination of the flame front's position, an average error of 0.3 mm on the flame tip position was assumed.

IGNITION, FLAME PROPAGATION AND FLASHBACK BEHAVIOR OF A N_2O AND C_2H_4 GREEN PROPELLANT

This error effects mainly the derived flame propagation speed during high velocities (small time steps) and results in the error bars shown in figure 6(a) and figure 8(a).

Further on the measurement data of the pressure sensors were compared to a calibrated reference device equipped with an Beamex EXT 250 pressure module. The thermocouple data was compared to the values of a calibrated Beamex FB660 Field Temperature Block. The maximum deviation of one of the pressure sensors in the investigated range was 2.35%, the maximum error of the Typ-K thermocouples was 2%.

The laminar flame speed calculation done with the optimized reaction mechanism and the cantera script was assumed to be in a $\pm 5\%$ range to the measured flame speeds. Those deviation of the flame speed caused the main part of the error bar in the Peclet number diagram (figure 11). The deviation of the pore size diameter could not be determined, the only available source was the data sheet of the manufacturer.¹⁸ It is assumed that the maximum pore size diameter is not always identical to the values given in the data sheet, but no reasonable approximation of the error could be done. Generally, the determination of the maximum or average pore diameter of a porous material seems to be a complicated undertaking.

To control and analyze the mixture ratio during the test campaign, gas samples of the combustible mixture were taken before and after a test series. The gas samples were analyzed via gas chromatography. The results are shown in figure 12. The average mixture ratio was $\Phi = 0.9$, while one sample showed a big deviation to a fuel rich composition.

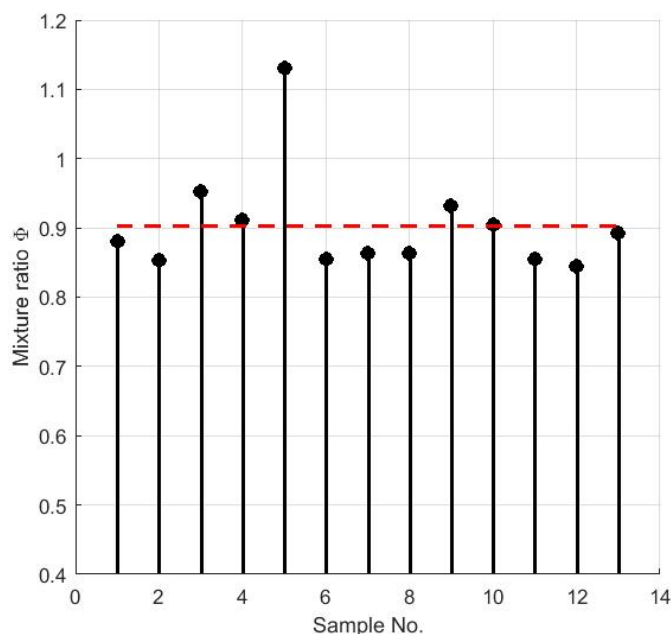


Figure 12: Deviation of mixture ratio during test campaign

During this test series, the mixing procedure was not done correctly (one valve was forgotten to close). The results of those test series were discarded. Additionally the samples taken at the end of a test run showed slight pollution with unknown gases. The chemical composition of those other gases was not examined, but it is very likely that those gases are combustion products from the previous test.

5. Summary and Outlook

Combustion and ignition tests with a gaseous mixture of N_2O (dinitrogen monoxide) and C_2H_4 (ethylene) at $\Phi = 0.9$ were conducted. The mixture was ignited via spark plug in a closed volume. The test setup consisted of two chambers an ignition chamber and a flashback chamber. In between the two chambers flashback arresting porous materials could be mounted. The ignition chamber is equipped with an quartz glass window to observe the flame propagation under different test conditions. The ignition and flame propagation was filmed for test cases with and without porous materials by a high speed camera. The high speed imaging data were used to derive the observed flame propagation speed. This velocity results form the laminar flame speed S_L and the expansion speed S_{exp} of the burned gases. During the experiments, the flame propagation speed was in the range 20-120 m/s. Furthermore pressure and temperature readings were taken during the ignition and flame propagation process. The pressure and temperature data were used

IGNITION, FLAME PROPAGATION AND FLASHBACK BEHAVIOR OF A N₂O AND C₂H₄ GREEN PROPELLANT

to determine if a flashback occurred during the tests with porous materials. For the flashback tests, the ignition pressure was raised step by step until a flame flashback was observed. In case of quenching or flashback Peclet numbers were calculated for the used sintered stainless steel materials (SIKA R) and the sintered bronze materials (SIKA B). To calculate the Peclet number the porous material's pore size, the laminar flame speed obtained from optimized reaction mechanisms and the thermal diffusivity from Refprop database were used. For the tested SIKA B material the critical quenching Peclet number is below 20, apart from one material which could not be tested up to the flashback limit. The tests with SIKA R material show critical peclet numbers above 40.

Two phenomena were observed:

First, the quenching ability of the porous materials seems to dependency on the length of the material. For the 7 mm long SIKA R 200 material, the critical Peclet number was above 40, for the 10.5mm long SIKA R 200 material, the critical Peclet number is above 80.

Second, the sintered bronze SIKA B materials quenches the flame not as sufficient as the sintered stainless steel material with comparable pore size. The quenching Peclet numbers for the bronze material are in between 1/2 to 1/4 of the numbers for the stainless steel material. The difference in between the two materials might be caused by catalytic effects of the bronze material.

For future tests the following modifications at the test setup are planned:

A vacuum pump should be mounted at the test setup to evacuate the test chamber prior to each single test and avoid pollution with burnt gas. The pressure transducers will be mounted directly at the combustion chamber walls. To investigate quenching at higher pressure levels, the chamber should be reconstructed, the sealing concept will also be rethought. For better comparability, capillary tubes with a defined diameter should be tested. Finally an image processing routine in Matlab will be developed to derive the flame propagation speed from the video data.

6. Acknowledgments

The authors would like to thank the M11 test bench team for the support in preparing and conducting the tests. Furthermore the help of the colleagues from the DLR institute of combustion technology, Torsten Methling and Clemens Naumann are greatly acknowledged. The work described in this paper was conducted in the framework of DLR's Future Fuels project.

References

- [1] Kjell Anflo and Crowe B. Two years of in-space demonstration and qualification of an ADN-based propulsion system on PRISMA. In *47th AIAA/ASME/SAE/ASEE Joint Propulsion Conference, 31. July-03 August 2011, San Diego, California, USA*.
- [2] Kjell Anflo and R. Möllerberg. Flight demonstration of new thruster and green propellant technology on the PRISMA satellite. *Acta Astronautica*, 65(9-10):1238–1249, 2009.
- [3] M. Bellenoue, T. Kageyama, S. A. Labuda, and J. Sotton. Direct measurement of laminar flame quenching distance in a closed vessel. *Experimental Thermal and Fluid Science*, 27(3):323–331, 2003.
- [4] Vittorio Bombelli, Dieter Simon, Jean-Luc Moerel, and Ton Marée. Economic Benefits of the Use of Non-Toxic Mono-Propellants for Spacecraft Applications: AIAA 2003-4783. In *39th AIAA/ASME/SAE/ASEE Joint Propulsion Conference 20-23 July 2003, Huntsville, Alabama, USA*.
- [5] B. Boust, J. Sotton, S. A. Labuda, and M. Bellenoue. A thermal formulation for single-wall quenching of transient laminar flames. *Combustion and Flame*, 149(3):286–294, 2007.
- [6] Ognjan Božić, Dennis Portmann, Daniel Lancelle, and Stefan May. Enhanced development of a catalyst chamber for the decomposition of up to 1.0 kg/s hydrogen peroxide. *CEAS Space Journal*, 8(2):77–88, 2016.
- [7] Angelo Cervone, Lucio Torre, Luca d'Agostino, Antony J. Musker, Graham T. Roberts, Cristina Bramanti, and Giorgio Saccoccia. Development of Hydrogen Peroxide Monopropellant Rockets. In *42nd AIAA/ASME/SAE/ASEE Joint Propulsion Conference & Exhibit, 9.-12. July 2006, Sacramento, California, USA*.
- [8] G. Ciccarelli. Explosion propagation in inert porous media. *Philosophical transactions. Series A, Mathematical, physical, and engineering sciences*, (370):647–667, 2012.
- [9] Christophe Clanet and Geoffrey Searby. On the “tulip flame” phenomenon. *Combustion and Flame*, (105):225–238, 1996.

IGNITION, FLAME PROPAGATION AND FLASHBACK BEHAVIOR OF A N₂O AND C₂H₄ GREEN PROPELLANT

- [10] J. Daou and M. Matalon. Influence of conductive heat-losses on the propagation of premixed flames in channels. *Combustion and Flame*, 128(4):321–339, 2002.
- [11] David G. Goodwin and Harry K. Moffat and Raymond L. Speth. CANTERA: An object-oriented software toolkit for chemical kinetics, thermodynamics, and transport processes, 2016.
- [12] E. W. Lemmon and M. L. Huber and M. O. McLinden. NIST Standard Reference Database 23: Reference Fluid Thermodynamic and Transport Properties-REFPROP, 2013.
- [13] European Chemicals Agency. Candidate List of substances of very high concern for Authorisation: published in accordance with Article 59(10) of the REACH Regulation, , <http://echa.europa.eu/en/candidate-list-table;>, 12.01.2017.
- [14] Mahdi Faghiih and Zheng Chen. The constant-volume propagating spherical flame method for laminar flame speed measurement. *Science Bulletin*, 61(16):1296–1310, 2016.
- [15] Colin R. Ferguson and James C. Keck. On laminar flame quenching and its application to spark ignition engines. volume 28, pages 197–205, 1977.
- [16] Valencia-Bel Ferran and Matthew Smith. Replacement of Conventional Spacecraft Propellants with Green Propellants. In *Space Propulsion Conference 7.-10 May 2012, Bordeaux, France*.
- [17] Jassin Fritz. *Flammenrückschlag durch verbrennungsinduziertes Wirbelaufplatzen*. Dissertation, München, Technische Universität, 2003-01-01.
- [18] GKN Sinter Metals. Filter-Elements High porosity sintered parts SIKA-R...AX and SIKA-B.
- [19] Amir S. Gohardani, Johann Stanojev, Alain Demairé, Kjell Anflo, Mathias Persson, Niklas Wingborg, and Christer Nilsson. Green space propulsion: Opportunities and prospects. *Progress in Aerospace Sciences*, 71:128–149, 2014.
- [20] Ulrich Gotzig, Stephan Kraus, Dietmar Welberg, Daniel Fiot, Pierre Michaud, Christian Desaguier, Santiago Casu, Bastian Geiger, and Rainer Kiemel. Development and Test of a 3D printed Hydrogen Peroxide Flight Control Thruster. In *51st AIAA/SAE/ASEE Joint Propulsion Conference, 27.-29. July 2015, Orlando, Florida, USA*.
- [21] Stanley S. Grossel. *Deflagration and detonation flame arresters*. CCPS concept book. Center for Chemical Process Safety of the American Institute of Chemical Engineers, New York, 2002.
- [22] Irvin Glassman and Richard A. Yetter, Irvin Glassman, Nick Glumac, and Richard A. Yetter. *Combustion*. Elsevier and Academic Press, Amsterdam, fourth edition, 2008.
- [23] Józef Jarosiński. Flame quenching by a cold wall. *Combustion and Flame*, 50:167–175, 1983.
- [24] H. I. Joo, K. Duncan, and G. Ciccarelli. Flame-Quenching Performance of Ceramic Foam. *Combustion Science and Technology*, (178):1755–1769, 2006.
- [25] Jozef Jarosinsky and Bernard Veyssiere. *Combustion phenomena: Selected mechanisms of flame formation, propagation, and extinction*. CRC Press, Boca Raton, 2009.
- [26] T. Katsumi, T. Inoue, J. Nakatsuka, K. Hasegawa, K. Kobayashi, Sh. Sawai, and K. Hori. HAN-based green propellant, application, and its combustion mechanism. *Combustion, Explosion, and Shock Waves*, 48(5):536–543, 2012.
- [27] Kenneth K. Kuo. *Principles of Combustion*. Wiley, Hoboken, NJ, 2. ed. edition, 2005.
- [28] Lukas Werling, Steffen Müller, Andreas Hauk, Helmut Ciezki, and Stefan Schleichriem. Pressure Drop Measurement of Porous Materials: Flashback Arrestors for a N₂O/C₂H₄ Premixed Green Propellant. In *52nd AIAA/SAE/ASME Joint Propulsion Conference, 25.-27. July, Salt Lake City, Utah, USA*.
- [29] Gregory Mungas, M. Vozoff, and B. Rishikof. NOFBX: A new non-toxic, Green propulsion technology with high performance and low cost: 63rd International Astronautical Congress. In *63rd International Astronautical Congress, 1-5 October 2012, Naples, Italy*.

IGNITION, FLAME PROPAGATION AND FLASHBACK BEHAVIOR OF A N₂O AND C₂H₄ GREEN PROPELLANT

- [30] N. Peters. Fifteen Lectures on Laminar and Turbulent Combustion: Ercoftac Summer School, 14.-28. September, 1992, Aachen Germany.
- [31] Michele Negri. Replacement of Hydrazine: Overview and First Results of the H2020 Project Rheform. In *6th European Conference for Aeronautics and Space Sciences (EUCASS), 29.06-03.7.2015, Krakow, Poland*.
- [32] Nobuyuki Azuma, Keiichi Hori, Toshiyuki Katsumi, Rachid Amrousse, Taiichi Nagata, Keigo Hatai, Teiu Kobayashi, Yoshio Nakayama, Tomoharu Matsumura, and Shuzo Fujiwara and Hidefumi Shibamoto. Research and Development on Thrusters with HAN (Hydroxyl Ammonium Nitrate) Based Monopropellant. In *5th European Conference for Aeronautics and Space Sciences, 1-5 July 2013, Munich, Germany*.
- [33] Randy Lillard. Technology Demonstration Missions Program: NASA Presentation: <https://www.nasa.gov/sites/default/files/files/RLillard.pdf>, 30.07.2013.
- [34] Robert S. Jankovsky. HAN-Based Monopropellants Assessment for Spacecraft: NASA Technical Memorandum 107287: AIAA-96-2863.
- [35] J. J. F. Scholten and J. A. Konvalinka. Reaction of nitrous oxide with copper surfaces. Application to the determination of free-copper surface areas. *Transactions of the Faraday Society*, 65:2465, 1969.
- [36] G. P. Smith, Golden, D. M. Frenklach, M., N. W. Moriarty, B. Eiteneer, M. Goldenberg, C. T. Bowman, R. K. Hanson, S. Song, W. C. Gardiner, V. V. Lissianski, and Z. Qin. GRI-Mech 3.0: http://www.me.berkeley.edu/gri_mech/.
- [37] Space.com. At Solar System's Edge, Old Voyager 1 Probe Performs New 'Acrobatics': <http://www.space.com/11087-nasa-voyager-1-acrobatics-solar-system.html>, 2011.
- [38] D. B. Spalding. A theory of inflammability limits and flame-quenching. *Proceedings of the Royal Society of London A: Mathematical, Physical and Engineering Sciences*, 240(1220):83–100, 1957.
- [39] R. STARKE and P. ROTH. An experimental investigation of flame behavior during cylindrical vessel explosions. *Combustion and Flame*, 66(3):249–259, 1986.
- [40] R. STARKE and P. ROTH. An experimental investigation of flame behavior during explosions in cylindrical enclosures with obstacles. *Combustion and Flame*, 75(2):111–121, 1989.
- [41] Th. Kick, J.H. Starcke, and C. Naumann. Green Propellant Substituting Hydrazine: Investigation of Ignition Delay Time and Laminar Flame Speed of Ethene / Dinitrogen Oxide Mixtures. In *8th European Combustion Meeting, 18. - 21. April 2017, Dubrovnik, Croatia*.
- [42] Stephen R. Turns. *An introduction to combustion: Concepts and applications*. McGraw-Hill series in mechanical engineering. McGraw-Hill, Boston, 2nd ed. edition, op. 2000.
- [43] Mark Ventura, Eric J. Wernimont, Stephen Heister, and Steve Yuan. Rocket Grade Hydrogen Peroxide (RGHP) for use in Propulsion and Power Devices - Historical Discussion of Hazards. In *47th AIAA/ASME/SAE/ASEE Joint Propulsion Conference, 31. July - 03. August 2011, San Diego, Californai, USA*.
- [44] Lukas Werling, Nikolaos Perakis, Benjamin Hochheimer, Helmut K. Ciezki, and S. Schleichriem. Experimental Investigations based on a Demonstrator Unit to analyze the Combustion Process of a Nitrous Oxide/Ethene Premixed Green Bipropellant. In *5th CEAS Air & Space Conference, 7.-11. Sept. 2015, Delft, Netherlands*.
- [45] Lukas Werling, Nikolaos Perakis, Steffen Müller, Andreas Hauk, Helmut Ciezki, and Stefan Schleichriem. Hot firing of a N₂O/C₂H₄ premixed green propellant: First combustion tests and results. In *Space Propulsion Conference, 1.-5. May 2016, Rome, Italy*.